THE EFFECT OF SOLUTE ATOMS ON GRAIN BOUNDARY MIGRATION, A SOLUTE PINNING APPROACH

E. Hersent, K. Marthinsen and E. Nes

Norwegian University of Science and Technology (NTNU), Department of Materials Science and Engineering, 7034 Trondheim, Norway

ABSTRACT

The effect of solute atoms on grain boundary migration has been modelled on the basis of the idea that solute atoms will locally perturb the collective re-arrangements of solvent atoms associated with boundary migration. The consequence of such perturbations is cusping of the boundary and corresponding stress concentrations on the solute atoms which will promote thermal activation of these atoms out of the boundary. This thermal activation is considered to be the rate-controlling mechanism in boundary migration. It is demonstrated that the present statistical approach is capable of explaining, in phenomenological terms, the known effects of solute atoms on boundary migration. The experimental results on the effect of copper on boundary migration in aluminium, due to Gordon and Vandermeer, have been well accounted for.

1. INTRODUCTION

It has been known for a long time that impurity solid solution atoms have a tendency of segregation to grain boundaries, an effect which may strongly retard the grain boundary mobility and thus the kinetics of recrystallization and grain growth in pure metals, even when present in the ppm range. The first quantitative treatment of this phenomenon, usually referred to as solute drag, was presented by Lucke and Detert [1], where they concluded that the effect is due to a direct interaction between the solute atoms and the moving grain boundaries.

Since the first quantitative treatment of Lucke and Detert, two main theoretical approaches of the solute drag effect on grain boundary mobility have come to dominate the literature. These are the treatments of Cahn [2] (commonly referred as the solute drag force approach) and Hillert [3] (commonly referred as the dissipation approach). Typical application examples for the force and dissipation approach are respectively [4-5] and [6]. In the force approach the solute drag is estimated by summing the forces that the solute atoms exert on the boundary and in the dissipation approach by evaluating the amount of free energy dissipated due to diffusion when the boundary goes through a volume containing one mole of material. Over the last decades, a lot of efforts have been made to generalize these approaches to a migrating phase boundary into a multi-component system [3, 7-9]. Indeed in the initial treatment of the solute drag effect by Cahn and by Lücke and Stüwe [10] the equation used for evaluating the solute drag does not apply to phase transformations. It only applies to the migration of grain boundaries, i.e. to one phase materials.

The force approach and the dissipation approach have both a sound physical basis and should therefore be equivalent. However the formula for calculating the solute drag for a migrating phase boundary into a multi-component system in steady-state conditions has been a subject of debates over the years and it was only recently that a valid expression has been found with a remarkable amount of empirical insight [11]. The general expression has also been derived in a deductive and completely independent way by applying the principle of maximum dissipation in [12].

Even if in the recent years more complex situations than the one treated in the initial works of Cahn [2] and Lücke and Stüwe [10] could be tackled, as two different types of solute [13-14], curved interfaces [15], solute drag occurring in a regular solid solution [16], during massive phase transformations [12, 17-20] or in non-steady state condition [21-22], they rely on the same framework: the composition profile of the solute atoms around the migrating phase boundary is calculated by solving Fick's law for diffusion and then the solute drag stems from the solute profile by applying the appropriate equation. In

this paper, however we will limit our discussion to the initial case treated by Cahn [2] and Lücke and Stüwe [10]: a moving grain boundary in a binary solid solution which is supposed ideal.

2. BACKGROUND THEORIES

The classical treatment. Lücke and Detert [1] were the first to present a quantitative theory of grain boundary mobility which took into account the interaction between the grain boundary and solute atoms. Their approach was further developed by Cahn [2] and Lücke and Stüwe [10, 23], to be refereed to as the CLS-theory. This theory rests on the assumption that a solute atom near a grain boundary interacts with the boundary, the interaction force being:

$$F(x) = -\frac{dU(x)}{dx} \tag{1}$$

where x is the distance between the solute atom and the boundary and $U(x)$ is the free energy of interaction. For a boundary at rest this interaction will result in a symmetrically shaped solute concentration profile across the boundary region. For dilute alloys (solute concentrations $c<<1$) it follows from Boltzmann-statistics that the boundary concentration c_b becomes:

$$c_b = c \exp\left(-\frac{U(x)}{kT}\right) \tag{2}$$

where $U(x=0) = -U_0$, T is the temperature and k is Boltzmann's constant. If a pressure P causes the boundary to migrate at a rate v_b, a consequence of this migration will be a redistribution of the solute concentration in the vicinity of the boundary. This solute atom redistribution will result in a net dynamic drag force P_s opposing the migration. And it follows from the treatment of Lücke and Stüwe [10] that the boundary migration rate becomes:

$$v_b = m(P - P_s) \tag{3}$$

where m is the intrinsic boundary mobility (i.e. that corresponding to $c = 0$). The treatments by Cahn [2] and Lücke and Stüwe [10, 23] are derived on the basis of the assumption that the effects on boundary mobility due to the cusp-formation resulting from the solute-boundary interaction can be neglected, the validity of this assumption is discussed below in this section. Another necessary assumption in order to derive Eq. (3) is that a migrating boundary in a solute containing metal can be assigned a mobility equal to that of the boundary in the pure metal. Or in other words, that the diffusivity of solute atoms across the boundary is approximately equal to that of the solvent ones. The

consequence of relaxing this latter assumption has been addressed by Westengen and Ryum [24]. They demonstrated that by assuming different boundary diffusion coefficients for solute and solvent atoms, a drag force of similar nature to that introduced above will result even if $U(x)$=0 for all values of x.

An important question to be addressed in the following becomes: is it acceptable, as proposed by Lücke and Stüwe [10], to reduce the effect of solute atoms on grain boundary migration into a drag only, ignoring the effects due to *in-situ* interactions between solute atoms and the boundary? This question will be tried answered below by considering the phenomenon of solute induced cusping of a migrating boundary. Firstly, however, the main predictions and the general applicability of the CLS-theory will briefly be considered.

Theory vs. experimental results. In qualitative terms the CLS-theory predicts that a grain boundary, subjected to a driving pressure (in a solute containing alloy), will migrate at a rate which will depend on solute concentration, driving pressure and temperature as schematically outlined in Fig. 1 a-c respectively. A characteristic feature displayed in these diagrams is the discontinuous speed changes commonly referred to as break-away or loading phenomena. For instance, by increasing the solute content, Fig. 1a, the drop is caused by a discontinuous increase in the boundary solute content (loading), while by increasing the pressure, Fig 1b, the rapid increase in speed is caused by a discontinuous decrease in solute content (break-away). However, these loading/break-away phenomena are not so precisely defined as that shown by the fully drawn curves in Fig 1. Rather, the CLS-theory predicts an S-shaped behaviour as indicated by the broken lines. The physical interpretation of this effect is that within these S-regions, where the theory has no unique solution, a general state of boundary solute instability exists. Only in the extreme cases, the CLS-theory is capable of quantitative predictions: for low solute contents, high driving pressures, high temperature situations there is no solute effect or the boundary is free and has the property of that in the pure metal, while in the other extreme of a loaded boundary this theory predicts a migration rate as given by:

$$v_b = \Gamma b \nu_D c^{-1} \left(\frac{Pb^3}{kT} \right) \exp\left(-\frac{U_s + U_o}{kT} \right) \qquad (4)$$

where the concentration c is given as atomic fraction, U_s is the activation energy for solute diffusion, b is a typical inter-atomic spacing, ν_D is the Debye frequency and Γ is a constant.

This relationship was derived for the first time by Lücke and Detert [1]. While the CLS-theory seems to provide a reasonable description, as shown above (Fig. 1), of the effects of solute atoms on grain boundary mobility, there are important aspects which are not satisfactorily covered. The following three comments seem relevant in this context. Firstly, in the low solute regime where a break-away situation predicts no solute-boundary interaction, the classic experiments of Aust and Rutter [25-28] do indicate the existence of such an effect as illustrated in Fig. 2. Secondly, within the relatively broad instability region of the CLS-theory where no predictions can be made, experimental investigations reveal no similar scatter in migration rate observations as also evident from Fig. 2 or in other words, reproducible results can be obtained even in regions of rapidly changing migration rates. Thirdly, for solute atoms which have activation energies of diffusion (within the boundary) different from that of the solvent atoms, a solute effect on boundary mobility is to be expected even if the interaction energy U_o is negligible or zero [24], in contrast to the prediction of the CLS-theory.

Boundary pinning. Machlin [29] considered that a moving grain boundary should become cusped at a point where it meets a solute atom, Fig. 3a, and he derived an expression for the pinning force by applying a Zener-drag type analysis. He supposed that the rate-controlling step in the migration process was diffusion of impurity atoms along the cusped parts of the boundary. Lücke and Stüwe [23] also considered this effect of cusping, but they concluded that the Zener-drag treatment was not very satisfactory from a theoretical point of view. It requires that the thickness of the boundary is small in comparison with the diameter of the solute atom, Fig. 3b, where, as argued by Lücke and Stüwe, for an individual solute atom just the opposite is true, Fig. 3c. Lücke and Stüwe's conclusion is probably correct in terms of the applicability of a Zener-drag type analysis in order to obtain the pinning action of individual solute atoms on a migration boundary. On the other hand, even if a Zener type analysis has to be rejected, it does not necessarily follow from such a conclusion that the solute cusping effect is insignificant or can be ignored. Roy and Bauer [30] were thinking along similar lines when suggesting a two-dimensional model where diffusion both parallel and perpendicular to the boundary were considered in terms of causing non-uniform solute distribution and associated shape changes and clustering. Their model indicated that clustering of impurities in the boundary and subsequent break-away of the boundary from the clusters are natural consequences of grain boundary migration.

The objective of the following treatment is to reconsider the Machlin idea that solute-atom-cusping will retard the migration of grain boundaries. The approach taken, however, differs from that of both Machlin [29] and Roy and Bauer [30]. The main effect of cusping in the present treatment is assumed

to be “stress-concentration” on the cusp-forming atoms and a corresponding change in the activation volume associated with the thermal activation of these atoms.

3 THE EFFECT OF SOLUTE PINNING ON BOUNDARY MIGRATION

3.1 General considerations

The migration of a high angle grain boundary in a pure metal has been treated in terms of different approaches, a review of which has been given by Humphreys and Hatherly [31]. All treatments, however, assume that if a pressure, *P*, acts on a boundary it will migrate at a rate:

$$v_b = mP = \Gamma_p b \nu_D \frac{Pb^3}{kT} \exp\left(-\frac{U_{SD}^b}{kT}\right) \tag{5}$$

In this equation Γ_p is a constant and U_{SD}^b is an activation energy associated with boundary migration. This activation energy is typically found to have a value half that of self-diffusion.

If solute atoms are added to the metal the situation will change. These atoms will interact with both a stationary and a migrating boundary as defined by Eq (1). The present treatment assumes a boundary region potential for the boundary-solute interaction as schematically outlined in Fig. 4a. i.e. $U(x) = -U_0$ for $(x(t) - \frac{\lambda}{2}) \le x(t) \le (x(t) + \frac{\lambda}{2})$ and $U(x)=0$ for all other values of x, where $x(t)$ is the instantaneous position of the boundary and λ its thickness. Outside the boundary region thermal activation of the solute atoms is associated with an energy U_s (i.e. that of solute bulk diffusion) except for jumping into the boundary where the activation barrier may be somewhat less (U_s^* in Fig. 4a), however, such an energy-profile-refinement will not be included in the present treatment at this stage. It follows that in the static case, Fig. 4a, the solute atom concentration in the boundary will be given by Eq. (2).

If a pressure acts on the boundary the boundary may start to migrate and this boundary concentration will change. In the present model the basic idea is that the effect of the solute atoms on the boundary migration rate will be determined by the rate at which such atoms are activated out of the boundary region. The pressure *P* driving the boundary, results in a cusping force F_C on each solute atom which reduces the activation barrier out of the boundary by $F_C b$ as illustrated by the "jumping out of the boundary" energy profile in Fig. 4b. To calculate the size of this pinning force F_C in mechanical terms requires a breaking-angle analysis, and as demonstrated by Lücke and Stüwe [23] the conclusions

which can be drawn from such an analysis are uncertain, indeed. In the present treatment, however, F_C is calculated in a different way making such an analysis unnecessary, see below.

The presence of the work-term, $F_C b$, may influence the boundary migration rate as qualitatively described in the following: imagine a situation where a pressure *P* is applied on a statically saturated boundary at time *t=0.* On the assumption of a dilute solid solution, the boundary regions far away (in terms of atomic dimensions) from boundary solute atoms will respond by migrating at a rate as determined by Eq. (5). Such a migration of the boundary is inhibited at the solute atom sites with the consequence that these atoms cusp the boundary. Let us assume, for a moment, that these atoms have an infinite interaction energy with the boundary, in which case the boundary bulges out until the local curvatures generated counter-balance the applied pressure. If, on the other hand, the boundary solute atoms are associated with a local energy situation as illustrated by the "jumping out of the boundary" energy profile in Fig. 4b, one alternative becomes an unpinning of the cusps by thermal activation of solute atoms out of the boundary (evaporation into the lattice), another alternative becomes un-cusping by boundary re-arrangements of solvent atoms. Which of these mechanisms will be rate controlling is difficult to decide, but will depend on the effect a solute atom has on the local collective solvent atom re-arrangements associated with boundary migration. *However, the present treatment of solute boundary interaction rests on the postulate that the first alternative above, i.e. "cusping-pressure-biased" thermal activation of boundary solute atoms out of the boundary, is the rate controlling step for the migration of the boundary*. The objective of the following becomes to explore the consequence of such a thermal activation mechanism on grain boundary migration in dilute solid solutions. This approach represents a 2D-analogy to similar treatments for the corresponding 1D-situation, i.e. migration of dislocations where solute pinning may control the migration rate, see Hirth and Lothe [32].

3.2 The model

Consider a boundary which migrates due to a constant driving pressure *P*. Some time after the pressure *P* has been applied a steady state boundary solute concentration c_b will be established, to which corresponds a steady state boundary migration rate v_b. This steady state solute concentration will be defined by

$$\phi^- + \phi^+ = 0 \qquad (6)$$

where ϕ^- is the rate per unit area at which the solute atoms leave the boundary and ϕ^+ is the corresponding arrival rate. It should be noticed that only the atoms jumping behind the boundary contribute to the leaving rate ϕ^-. Indeed the atoms jumping forward will be immediately recaptured by the migrating boundary. Then the leaving rate ϕ^- is proportional to the backwards jump frequency out of the boundary ν^-:

$$\phi^- = c_b\, n_b \lambda \nu^- \tag{7}$$

where the boundary concentration c_b is given in terms of atomic fraction and n_b is the number of atoms per unit volume inside the boundary. Within the context of the schematic energy profiles in Fig. 4b the backwards jump frequency ν^- can be expressed, in terms of thermal activations, as follows:

$$\nu^- = \Gamma^- \nu_D \exp\left(-\frac{U_s + U_o - F_C b}{kT}\right) \tag{8}$$

with Γ^- a constant. The work $F_C b$ done by the force F_C decreases the energy barrier $U_s + U_0$ even if the atom does not jump in the direction of the force F_C because the displacement of the grain boundary releases the stress accumulated at the pinning atom. Finally the leaving rate is given by:

$$\phi^- = \Gamma^- c_b\, n_b \lambda \nu_D \exp\left(-\frac{U_s + U_0 - F_C b}{kT}\right) \tag{9}$$

The arrival rate ϕ^+ can be written as follows

$$\phi^+ = -\left[\Gamma^+ cnb\nu_D \exp\left(-\frac{U_s}{kT}\right) + cn\mathrm{v}_b\right] \tag{10}$$

where c is the bulk solute concentration (in atomic fraction), n the number of atoms per unit volume in the bulk of the material and Γ^+ is a constant. The first term in Eq. (10) represents thermal activation of bulk atoms into the boundary and the second "sweeping term" reflects the constant flux of solute atoms arriving in the boundary due to its migrating at a rate v_b into a lattice containing a solute concentration c.

Balancing the expressions for ϕ^+ and ϕ^- (Eq. (6)) makes it possible to calculate $c_b(c, T, F_C)$, provided an expression for the boundary migration rate $\mathrm{v}_b(c, T, F_C)$ is obtained. A characteristic of a steady state conditions (Eq. (6)) is that when a solute atom 'evaporate' from the grain boundary another necessarily will arrive and pin it again. Consequently, as a statistical average, the distance the boundary will move

in-between thermal activation and repinning typically becomes an atomic distance of size *b*. And it follows that in terms of thermal activations the boundary speed can be written:

$$\mathrm{v}_b = b\left[\nu^- - \Gamma^- \nu_D \exp\left(-\frac{U_s + U_0 + F_C b}{kT}\right)\right] \tag{11}$$

The second term inside the parenthesis is required in order to take into account the statistical probability that solute atoms may jump against the cusping induced bias, $F_C b$, as illustrated schematically in Fig. 5. So a solute atom has to overcome an energy barrier equals to the energy barrier when there is no cusping effect $U_s + U_0$ plus the necessary energy $F_C b$ to compensate for the work done by the force F_C during the backward jump, as illustrated by the "jumping with the boundary" energy profile in Fig. 4b. In this case the solute atom will remain in the boundary and consequently the jump has no effect on the ν^--term. Similar backwards jumps are also included in Hirth and Lothe's treatment of solute drag of moving dislocations [32].

Combination of Eqs. (8) and (11) gives the following expressions for the boundary velocity v_b:

$$\mathrm{v}_b = 2\Gamma^- b \nu_D \exp\left(-\frac{U_s + U_0}{kT}\right)\sinh\left(\frac{F_C b}{kT}\right) \tag{12}$$

and by combining this relationship with Eq. (10) an expression for ϕ^+ is obtained and it then follows from Eq. (6), that the boundary solute concentration c_b can be written:

$$c_b = c\frac{n b}{n_b \lambda}\exp\left(\frac{U_0 - F_C b}{kT}\right)\left[1 + 2\left(\exp\left(-\frac{U_0}{kT}\right)\right)\sinh\left(\frac{F_C b}{kT}\right)\right] \tag{13}$$

In deriving this expression the constants Γ^- and Γ^+ have been assumed to be of approximately the same size and have consequently been represented by a common symbol, Γ_s, in the following. It is easily seen that Eq. (13) is consistent with the required boundary conditions that for low driving pressures/high solute concentrations, i.e. and $F_C b / kT << 1$, the boundary concentration becomes the

equilibrium level $c_b = c\exp\left(\frac{U_0}{kT}\right)$ assuming the ratio $\frac{n\,b}{n_b\lambda}$ nearly equal to 1, and for high pressures/low solute concentrations, i.e. $F_C b / kT \gg 1$, $c_b = c$, conditions referred to as loaded and break-away situations, respectively, in the solute drag theory.

In order to achieve complete solutions of Eq. (12) and (13), an expression for the pinning force F_C is needed, or more exactly for the ratio $\frac{F_C b}{kT}$. Fortunately it is possible to calculate this force because an alternative expression to Eq. (12) for the migration rate can be formulated. By having two independent relationships for the same migration rate the pinning force problem can be solved.

A second expression for the boundary speed is obtained by considering a boundary subjected to a driving pressure *P* and which also experiences a restraining pressure $P_C = F_C / A = F_C \lambda c_b n_b$, Fig. 4. In-between these restraining points the boundary is free of solute atoms with a mobility, *m*, typical of that of a pure metal, Eq. (5), and it follows that boundary speed now can be written:

$$\mathrm{v}_b = m\left(P - \frac{2\gamma}{R} - P_C\right) \tag{14}$$

with *R* the effective radius of the boundary curvature between the restraining points. The pressure stemming from the grain boundary curvature will be neglected in the following treatment, which assumes that the grain boundary remains macroscopically planar during its migration. It should be remarked that this treatment is different from that of Cahn and Lucke and Stüwe [2, 10] where the relationship $\mathrm{v}_b = m\left(P - P_s\right)$ is applied regardless whether the grain boundary is free of solute atoms or not.

By equating the two expressions for the boundary migration rate, Eq. (12) and (14), and by replacing *m* by its expression Eq. (5) the pinning force is obtained. Unfortunately it is not possible to give this force in terms of an analytical expression, only an implicit expression can be given:

$$c = \frac{1}{nb^3}\frac{\left(\frac{Pb^3}{kT} - 2\frac{\Gamma_s}{\Gamma_p}\exp\left(-\frac{U_s + U_0 - U_{SD}^b}{kT}\right)\sinh\left(\frac{F_C b}{kT}\right)\right)\exp\left(\frac{F_C b}{kT}\right)}{\frac{F_C b}{kT}\left(\exp\left(\frac{U_0}{kT}\right) + 2\sinh\left(\frac{F_C b}{kT}\right)\right)} \tag{15}$$

However, by numerical treatments it becomes possible to calculate $F_C(c,P,T)$, $c_b(c,P,T)$ and $v_b(c,P,T)$ for any given combination of materials specific parameters n, b, c, Γ_p, Γ_s, U_{SD}^b, U_0, and U_s if it is assumed the ratio $\frac{nb}{n_b\lambda}$ close to 1. In computing the boundary solute concentration c_b and the migration rate v_b the size of the pinning force F_C is monitored in order to check that this force does not exceed that expected from a mechanical breaking-angle analysis. As argued by Lücke and Stüwe [23] such an analysis is very uncertain, but an estimate for the maximum possible force F_C is obtained from a Zener-drag type argument, i.e. $F_{\max} = \pi\gamma b$, where γ is the boundary energy. In the subsequent numerical treatment the pinning force F_C is always smaller, or much smaller than this maximum value, see also Appendix 1.

In the special case of a low driving pressure/high solute concentration, i.e. $F_C b / kT << 1$, a good approximate solution for the migration rate of a loaded boundary becomes:

$$v_b = \frac{2}{nb^3}\Gamma_s b \nu_D c^{-1}\left(\frac{Pb^3}{kT}\right)\exp\left(-\frac{U_s + 2U_0}{kT}\right) \tag{16}$$

where Γ_s is a constant. This expression for the boundary migration rate is, except for the numerical factors $\frac{2}{nb^3}$ and 2 in front of U_0, similar to Eq. 4, i.e. that was originally derived by Lücke and Detert [1]. The origin of the factor 2 in front of U_0 stems from that in the present model the interaction energy U_0 appears twice: (i) in the boundary solute concentration in the fully loaded case (Eq. (2)), and (ii) in the activation frequency of atoms jumping out of the boundary (Eq. (8)).

3.3 Model predictions

In contrast to the solute-drag theory the present analytical treatment is simple indeed. The predictions for the boundary solid solution contents c_b and the migration rates v_b for grain boundaries, acted upon by a pressure P in a generic solid solution alloy of various solute contents c, are illustrated qualitatively in Figs 6 a and b, respectively. The metal studied is assumed to have a close packed spacing b equal to 3 Å (typical value in metals). Then the atomic density n is estimated as $\frac{1}{b^3}$ and the ratio $\frac{nb}{n_b\lambda}$ as close to 1. The values of the input parameters used are given in Fig. 6a, except for the activation energy for

boundary migration U_{SD}^{b}, which for the sake of simplicity is taken as the half of the activation energy for solute diffusion U_S, and for the constants Γ_p and Γ_s for which numerical values *18* and *82* respectively, have been selected (the procedure adopted for the quantification of these parameters in an experimental case is explained below). Figure 6a shows the grain boundary concentration c_b as a function of the matrix concentration c for various values of the interaction energy U_o. The corresponding variation in the boundary migration rate v_b is illustrated in Fig. 6b. Note that for values of U_o larger than some critical level, the c_b vs. c curves become S-shaped, and consequently the v_b vs c curve takes the form of a similarly shaped configuration, broken lines in the figures. A similar behaviour is predicted also by the CLS-theory and is there interpreted as an instability phenomenon associated with either break-away or loading, see Section 1. The physics, however, behind this peculiar behaviour is more transparent in the present treatment where the break-away/loading phenomenon is reduced to a well defined discontinuity (fully drawn lines), the reason for which can be explained in free energy terms as follows: by increasing the c-values from the lower side in Fig. 6a one eventually reaches the point marked A where the system spontaneously can lower its free energy by a discontinuous increase in boundary concentration, point B, i.e. a concentration close to the equilibrium one defined by Eq. (2).

In terms of comparing the predictions which follow from the present solute pinning approach to that of the CLS-theory, two important differences emerge: (i) the present model predicts a c-dependence in the boundary migration rate, v_b also for c-values below the break-away level in accordance with experimental observations e.g. Fig. 2, in contrast to the CLS-theory, and (ii) a strong solute pinning effect may, according to the present approach, prevail even in cases where the interaction energy $U_o = 0$. It appears as intuitively obvious that in cases where the activation energy for solute diffusion in the boundary is significantly different from that of boundary self diffusion the solute atoms will disturb the solvent redistribution pattern and restrict boundary migration even if the "long range" elastic interaction is negligible. A similar U_0-effect is found in the model by Westengen and Ryum [24]. The effect of varying the main variables P and T on the boundary migration rate is illustrated in Figs 7a and 7b, respectively. While the CLS-theory is capable of making quantitative predictions only in the low pressure/high concentration/low temperature (fully loaded) regime, the present model gives equally good predictions for any combination of driving pressure, solute concentration and temperature, as will be demonstrated in the application section below.

4 APPLICATIONS

The present model will now be tested on the bases of some classical experimental investigations, of which the most notable ones are those due to Aust and Rutter [25-28] and Gordon and Vandermeer [33-36]. The latter work, on the effect of small additions of Cu on grain boundary migration in aluminium is the most carefully conducted experiment of its kind, and will therefore firstly be examined.

To allow some flexibility in the model a tuning parameter has been introduced. The area acted upon by the restraining pressure P_C was taken only as a fraction κ of the geometrical area A initially assigned:

$$a = \kappa A = \frac{\kappa}{c_b n_b \lambda} \tag{17}$$

The physical meaning is that the activation volume related to the work of the force F is actually smaller than the one predicted geometrically. This parameter modifies the restraining pressure in the following way $P_C = \frac{F_C}{a} = \frac{1}{\kappa} F_C c_b n_b \lambda$. The consequence of this takes the form of introducing κ as a multiplication factor in the right-hand side of Eq.(15) whereas the expressions for the boundary velocity v_b (Eq.(12)) and the boundary solute concentration c_b (Eq. (13)) in function of F_C are unaffected. It also slightly modifies the expression of the migration rate v_b of a loaded boundary (Eq.(16)) which now takes the form:

$$\mathrm{v}_b = 2\frac{\kappa}{nb^3}\Gamma_s b \nu_D c^{-1} \frac{Pb^3}{kT} \exp\left(-\frac{U_s + 2U_0}{kT}\right) \tag{18}$$

The experiments of Gordon and Vandermeer. These researchers investigated the effect of adding copper (range 2-250 ppm to zone refined aluminium) on grain boundary migration [33-36]. The experimental procedure adapted was to cold roll the various compositions to a reduction of 40% and subsequently follow the initial stage of recrystallization at various temperatures carefully monitoring *initial* growth rate of the largest grain. Great care was exercised in order to assure that this initial stage of growth in all investigated conditions occurred under constant driving pressure [36]. Their results, in terms of migration rates vs. solute concentration, are shown in Fig. 8. From these results it follows that in the extremes the boundary migration rates are well represented by Eqs. (5) and (18). Equation (5) applies to zone refined aluminium with an activation energy $U_{SD}^b = 65\,\mathrm{kJ/mol}$. The results in the ultimate (high concentration) range, satisfy Eq. (16) with $U_s + 2\,U_o$ = 131 kJ/mol. Further, it follows from the behaviour in these extremes that the two pre-exponential constants can be identified as:

$\Gamma_P = 2.5\,10^9/P$ and $\Gamma_s = 1.2\,10^{10}\kappa/P$. A test of the present model now becomes to find out if it is capable of accounting for the effect of solute atoms on boundary migration also in-between these extremes.

In order to apply the present model to the results in Fig. 8 the driving pressure involved needs to be quantified. Gordon and Vandermeer estimated the driving pressure on the basis of a relationship of the form: $P = 4Z / Na_o^3$, where Z is the stored free energy per mole, N is Avogadros number and a_o is the lattice parameter. On the basis of calorimetric measurements Z was estimated to 16.7 J/mol which gives P = 1.7 MPa, which again corresponds to a dislocation density estimate ($P = 0.5\,Gb^2\rho$, where G is the shear modulus and ρ is the dislocation density) at $\rho = 1.6*10^{15}$ m^{-2}. This is a high density, indeed, to be the result of a 40% rolling reduction of zone-refined-grades of aluminium. In terms of a shear flow stress estimate ($\tau = \tau_0 + 0.5Gb\sqrt{\rho}$) such a dislocation density corresponds to a stress level of about 150 MPa, which is about an order of magnitude larger than expected. In commercial 5N-grades of aluminium the shear flow stress (in multiple slip, at 40% elongation) is found to be about 15 MPa [37]. Typical value for τ_0 is about 5 MPa, which again gives the following estimates for the dislocation density and the stored energy: $\rho = 7*10^{12}$ m^{-2} and P = 7 500 Pa, respectively. Gordon and Vandermeer, however, investigated aluminium with Cu-contents in the atomic fraction range from $2\cdot10^{-6}$ to $3\cdot10^{-4}$. This variation in solute content will result in a corresponding variation in flow stress and driving pressure at a constant rolling reduction (see Table 1). This effect is illustrated in Fig. 9 where the driving pressure for three low-solute variants (5N, 4N and commercial purity aluminium) indicate an approximate power relationship in this solute regime. The model predictions illustrated in Fig. 8 are based on this driving pressure relationship. Note that this fit also requires $\kappa = 0,4$ and $U_0 = 3\,\mathrm{kJ/mol}$, from which it follows that the activation energy U_s becomes 125 kJ/mol, which is also a reasonable value, close to the activation energy for bulk diffusion of Cu in Al; 135 kJ/mol [38]. From the diagram in Fig. 8, v_b *vs. 1/T*-plots at constant concentrations can be generated, from which the theoretically predicted variation in the (partly apparent) activation energy in Fig. 10 is obtained. In contrast to what is observed no maximum in the apparent activation energy is predicted by the model. As this region does not correspond to a simple physical mechanism it is quite difficult to give an explanation to this discrepancy. The conclusion becomes that the present theory is able to adequately account for the Gordon and Vandermeer observations by means of a fitting parameter.

The experiments of Aust and Rutter. These experiments pertain to the effects of small additions of Ag, Au and Sn on grain boundary migration in melt grown single crystals of lead [25-28], the driving pressure for boundary migration in this case being the grown-in striation (subgrain) structure. The claimed advantage of this approach is the thermal stability of the substructure which assured a constant driving pressure through-out the experiment. How accurate this claim is will be further discussed below. The authors did mention, however, the problems of reproducing the striation structure from wire to wire, and of maintaining a constant structure along the wire. This problem probably explains the considerable scatter (a factor of 5) in the measured migration rates, especially for low solute contents, see Fig 2.

Let us firstly consider the results on the effect of Sn in Pb given in Fig. 11. The diagram gives the boundary migration rate as a function of Sn-concentration at 300 °C at a constant driving pressure *P*. By applying the modelling approach described above using $\kappa = 1$, $U_{SD}^{b} = 54\,\text{kJ/mol}$, $U_0 = 5\,\text{kJ/mol}$ and $U_s + 2U_0 = 100\,\text{kJ/mol}$ the pre-exponential factors become: $\Gamma_P = 4,410^5/P$ and $\Gamma_s = 218/P$. As can be seen from Fig. 11 the best fit is obtained with a driving pressure *P* = 15000 Pa. This value is more than two order of magnitude larger than the driving pressure estimate made by Aust and Rutter (400 Pa). Keeping this low driving pressure and adjusting the fitting parameter κ lead to an extremely high value ($\kappa = 32$), which seems unreasonable to adopt. However before considering the possible reasons for this discrepancy, some other observations on the effects of Sn on grain boundary migration in zone-refined lead needs to be brought to the attention. Some interesting results on grain growth due to Bolling and Winegard [39-40] are shown in Fig. 12. These results are often quoted as demonstrating that the effect of these solute elements on the boundary migration rate increases in the order Sn-Ag-Au. The effect of Sn is not included in Fig. 12, the reason being that these researchers apparently could not find any effect of Sn on grain growth at all. It is difficult to precisely quantify the driving pressure in grain growth experiments, but at a grain size of about 1 mm this pressure ($P \simeq 2\gamma_{GB}/R$ where γ_{GB} is the grain boundary energy and R the average grain radius) is expected to be of approximately the same order as in the experiments of Aust and Rutter. It is, however, very difficult to understand why an addition of around 100 ppm of Sn to Pb has only a marginal effect on grain growth, but causing a 4 orders of magnitude change in the migration rate in the experiments of Aust and Rutter, Fig. 11. A possible explanation will be offered below, but firstly the effects of the other solute additions need to be considered.

A total representation of the Aust and Rutter data is given in Fig. 2. Although the scatter in the Sn and Au data is considerable the trend seems clear, indicating a several orders of magnitude drop in boundary migration rate for solute concentration larger than a few ppm. Again, this is in total conflict with the grain growth observations by Bolling and Winegard [39-40], showing that the average growth rates at a grain size of 1 mm are $7\,10^{-6}$ m/s, $4\,10^{-6}$ m/s and $3\,10^{-6}$ m/s taken in the order pure Pb, Pb - Ag and Pb - Au (Fig 12). While the driving pressure in grain growth experiments is difficult to assess one cannot dispute the fact that these growth rates all refer to approximately the same driving pressure. An interesting speculation becomes to which extent the observations of Aust and Rutter really reflect a constant driving pressure or not. An important argument in favour of such a constant pressure has traditionally been that the striation structure is stable during the migration experiments. One has to bear in mind, however, that we are here talking about experimenting with single crystal wires, a few mm in radius and containing, according to Aust and Rutter, an average dislocation density of about $7*10^7$ m^{-2}, i.e. handling thin lead wires having a shear flow stress of about 0.5 MPa. Doing that without introducing dislocations in an amount many times larger than that grown in will be a problem in itself. Bolling and Winegard reported that as the solute content increased so did the flow stress of the material (of course). An interesting speculation then becomes whether or not by increasing the solute content the lead wires became stronger and easier to handle without introducing additional dislocations, and accordingly the drop in migration speed in Figs. 2 or 11 is partly due to a decrease in driving pressure. The works by Aust and Rutter provide no answer to such a speculation. It is, however, the opinion of the present authors that the observations of Bolling and Winegard cannot be overlooked in this context. They have convincingly demonstrated that the effects of additions of about 100 ppm of either Sn, Ag or Au on the grain boundary migration rates in zone-refined lead at a *constant* driving pressure caused migration speed reductions compared to the pure metal of at most a factor of 3. From these observations it seems appropriate to question the more spectacular results by Aust and Rutter in Figs. 2 and 11. The present conclusion then becomes that their results in general are not suited as a basis for applications in quantitative modelling.

5. CONCLUDING REMARKS

The solute pinning approach developed in the present paper rests on the assumption that solute atoms within a migrating boundary perturb the collective re-arrangements of solvent atoms associated with boundary migration, the consequence of which being cusping of the boundary and a pinning force on the solute atoms. This pinning force will promote thermal activation of solute atoms out of the boundary, a reaction which is believed to be the rate controlling step for grain boundary migration in

solute containing metals. It has been demonstrated that this mechanism is capable of explaining the known effects due to solute atoms on grain boundary migration in relation to recrystallization and grain growth phenomena. The experimental results on the effect of copper on boundary migration in aluminium due to Gordon and Vandermer [33-36] have been described successfully by this new model.

ACKNOWLEDGEMENTS

The authors would like to acknowledge the financial support from the Research Council of Norway KMB project No.193179/II40. A very special thank to Dr. O. Engler for useful discussions and help in solving the computational problems.

REFERENCES

1. K. Lücke and K. Detert: *Acta Metall.*, 1957, vol. 5, no.11, pp. 628-37.
2. J.W. Cahn: *Acta Metall.*, 1962, vol. 10, no.9, pp. 789-98.
3. M. Hillert and B. Sundman: *Acta Metall.*, 1976, vol. 24, no.8, pp. 731-43.
4. I. Andersen and Ø. Grong: *Acta Metall. Mater.*, 1995, vol. 43, no.7, pp. 2673-88.
5. L.M. Fu, H.R. Wang, W. Wang, and A.D. Shan: *Mat. Sci. Technol.*, 2011, vol. 27, no.6, pp. 996-1001.
6. M. Hillert and B. Sundman: *Acta Metall.*, 1977, vol. 25, no.1, pp. 11-18.
7. J. Ågren: *Acta Metall.*, 1989, vol. 37, no.1, pp. 181-89.
8. M. Enomoto: *Acta Mater.*, 1999, vol. 47, no.13, pp. 3533-40.
9. G.R. Purdy and Y.J.M. Brechet: *Acta Metall. Mater.*, 1995, vol. 43, no.10, pp. 3763-74.
10. K. Lücke and H.P. Stüwe: *Acta Metall.*, 1971, vol. 19, no.10, pp. 1087-99.
11. M. Hillert: *Acta Mater.*, 2004, vol. 52, no.18, pp. 5289-93.
12. J. Svoboda, J. Vala, E. Gamsjäger, and F.D. Fischer: *Acta Mater.*, 2006, vol. 54, no.15, pp. 3953-60.
13. Y.J.M. Bréchet and G.R. Purdy: *Acta Mater.*, 2003, vol. 51, no.18, pp. 5587-92.
14. M.I. Mendelev and D.J. Srolovitz: *Interface Sci.*, 2002, vol. 10, no.2-3, pp. 191-99.
15. A.L. Korzhenevskii, R. Bausch, and R. Schmitz: *Acta Mater.*, 2006, vol. 54, no.6, pp. 1595-96.
16. M.I. Mendelev and D.J. Srolovitz: *Acta Mater.*, 2001, vol. 49, no.4, pp. 589-97.
17. M. Hillert and M. Schalin: *Acta Mater.*, 2000, vol. 48, no.2, pp. 461-68.
18. R. Okamoto and J. Ågren: *Int. J. Mater. Res.*, 2010, vol. 10, pp. 1232-40.
19. J. Svoboda, E. Gamsjäger, F.D. Fischer, and P. Fratzl: *Acta Mater.*, 2004, vol. 52, no.4, pp. 959-67.
20. J. Svoboda, E. Gamsjäger, F.D. Fischer, Y. Liu, and E. Kozeschnik: *Acta Mater.*, 2011, vol. 59, no.12, pp. 4775-86.
21. J. Li, J. Wang, and G. Yang: *Acta Mater.*, 2009, vol. 57, no.7, pp. 2108-20.
22. J. Svoboda, F.D. Fischer, and M. Leindl: *Acta Mater.*, 2011, vol. 59, no.17, pp. 6556-62.
23. K. Lücke and H.-P. Stüwe: *Recovery and Recystallization of Metals*, ed. Himmel, Wiley, New York, 1963, pp.171-210
24. H. Westengen and N. Ryum: *Philos. Mag. A*, 1978, vol. 38, no.3, pp. 279-95.
25. K.T. Aust and J.W. Rutter: *Trans. AIME*, 1959, vol. 215, pp. 119.
26. K.T. Aust and J.W. Rutter: *Trans. AIME*, 1959, vol. 215, pp. 820.

27. K.T. Aust and J.W. Rutter: *Recovery and Recrystallization of Metals*, ed. Himmel, Wiley, New York, 1963, pp.131-59
28. J.W. Rutter and K.T. Aust: *Trans. AIME*, 1969, vol. 218, pp. 682.
29. E.S. Machlin: *Trans. AIME*, 1962, vol. 224, pp. 1153-67.
30. A. Roy and C.L. Bauer: *Acta Metall.*, 1975, vol. 23, no.8, pp. 957-63.
31. F.J. Humphreys and M. Hatherly: *Recrystallization and Related Annealing Phenomena*, second ed., Elsevier, Oxford, 2004, pp. 134-165.
32. J.P. Hirth and J. Lothe: *Theory of Dislocations*, Mc.-Graw-Hill, New York, 1968, pp. 639-640.
33. P. Gordon and R.A. Vandermeer: *Trans. AIME*, 1962, vol. 224, pp. 917-28.
34. P. Gordon and R.A. Vandermeer: *Recrystallization Grain Growth and Texture*, ASM, Ohio, 1966, pp. 205-66.
35. R.A. Vandermeer and P. Gordon: *Recovery and Recrystallization of Metals*, ed. L. Himmel, Wiley, New York, 1963, pp.211-40
36. R.A. Vandermeer and P. Gordon: *Trans. AIME*, 1959, vol. 215, pp. 577-88.
37. Ø. Ryen, B. Holmedal, O. Nijs, E. Nes, E. Sjölander, and H.-E. Ekström: *Metall. Mater. Trans. A*, 2006, vol. 37, no.6, pp. 1999-2006.
38. N.L. Peterson and S.J. Rothman: *Phys. Rev. B*, 1970, vol. 1, no.8, pp. 3264-73.
39. G.F. Bolling and W.C. Winegard: *Acta Metall.*, 1958, vol. 6, no.4, pp. 283-87.
40. G.F. Bolling and W.C. Winegard: *Acta Metall.*, 1958, vol. 6, no.4, pp. 288-92.

Appendix

The information contained in equation Eqs. (6)-(15) can be condensed into the following three analytical expressions:

$$c = \frac{\kappa}{nb^3}\frac{\left(\frac{Pb^3}{kT} - 2\frac{\Gamma_s}{\Gamma_p}\exp\left(-\frac{U_s + U_0 - U_{SD}^b}{kT}\right)\sinh(x)\right)\exp(x)}{x\left(\exp\left(\frac{U_0}{kT}\right) + 2\sinh(x)\right)}$$

$$c_b = c\frac{nb}{n_b\lambda}\exp\left(\frac{U_0}{kT}\right)\left(1 + 2\exp\left(-\frac{U_0}{kT}\right)\sinh(x)\right)\exp(-x)$$

$$\mathrm{v}_b = 2\Gamma_s b\nu_D \exp\left(-\frac{U_s + U_0}{kT}\right)\sinh(x)$$

where $x = \frac{F_C b}{kT}$ and κ the tuning parameter introduced in the application section. The computational procedure now becomes to find the value of x which satisfies the first equation and then the solute concentration in the boundary c_b and the interface velocity v_b could be deduced from the value of x found. It should be noted that the possible values of x are in the interval $[0, x_{\max}]$ where $x_{\max}$ is obtained from the necessary requirement that the nominator in the first equation has to be larger than 0. Making it equal to zero gives:

$$x_{\max} = \sinh^{-1}\left(\frac{1}{2}\frac{\Gamma_p}{\Gamma_s}\frac{Pb^3}{kT}\exp\left(\frac{U_s + U_0 - U_{SD}^b}{kT}\right)\right)$$

Expression of the interface velocity where $\frac{F_C b}{kT} \ll 1$:

This corresponds to the case of a low driving pressure or a high solute concentration. If the expression of c is expanded to the lowest order, we obtain:

$$c = \frac{\kappa}{nb^3}\frac{\frac{Pb^3}{kT}}{x\exp\left(\frac{U_0}{kT}\right)}$$

From this expression we simply get the value of x:

$$x = \frac{\kappa}{nb^3}\frac{\frac{Pb^3}{kT}}{c\exp\left(\frac{U_0}{kT}\right)}$$

By substituting the expression of x into the expression of the boundary velocity and using the approximation $\sinh(x) \approx x$ for small value of x, we easily obtain:

$$\mathrm{v}_b = 2\frac{\kappa}{nb^3}\Gamma_s b\nu_D c^{-1}\frac{Pb^3}{kT}\exp\left(-\frac{U_s+2U_0}{kT}\right)$$

It can also be easily demonstrated that $c_b \approx c\exp\left(\frac{U_0}{kT}\right)\frac{nb}{n_b\lambda}$.

It should be noted that in this case the pinning force could be expressed in an analytical way:

$$F_C = \frac{n_b\lambda}{nb}Pa$$

Everything behaves as if the grain boundary is planar: it is pinned in so many places that the curvature between two pinning atoms is small.

Expression of the interface velocity where $\frac{F_C b}{kT} \gg 1$

This corresponds to the case of high driving pressure or low solute concentration. In this case x is close to $x_{\max}$.

$$x \sim x_{\max} = \sinh^{-1}\left(\frac{1}{2}\frac{\Gamma_p}{\Gamma_s}\frac{Pb^3}{kT}\exp\left(\frac{U_s+U_0-U_{SD}^b}{kT}\right)\right)$$

The interface velocity is given by:

$$\mathrm{v}_b(x) \approx \mathrm{v}_b(x_{\max}) = b\Gamma_s\nu_D\exp\left(-\frac{U_s+U_0}{kT}\right)2\sinh(x_{\max})$$

$$\mathrm{v}_b(x) = \frac{\Gamma_p\nu_D b^4}{kT}\exp\left(-\frac{U_{SD}^b}{kT}\right)P$$

This expression is the same expression of the velocity of a pure boundary.

For $x \gg 1$, $\sinh(x) \approx \frac{e^x}{2} \gg 1$ and the solute concentration in the boundary c_b is given by:

$$c_b \approx c\exp\left(\frac{U_0}{kT}\right)\frac{nb}{n_b\lambda}2\frac{1}{2}\exp\left(-\frac{U_0}{kT}\right)\exp(x)\exp(-x)$$

$$c_b \approx c\frac{nb}{n_b\lambda}$$

For this case there is almost no segregation at the moving interface.

FIGURES

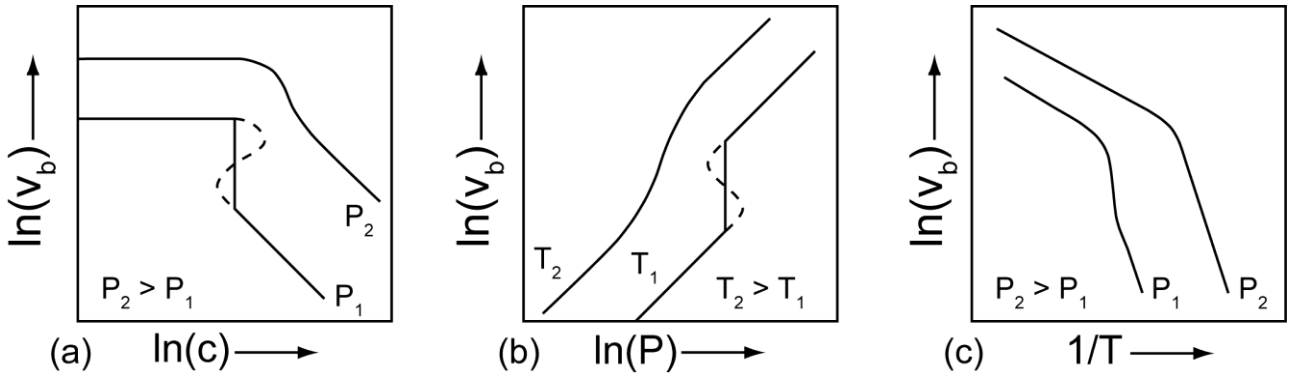

Fig. 1. Some possible types of transitions (schematically) from free to loaded boundary, for details see the text.

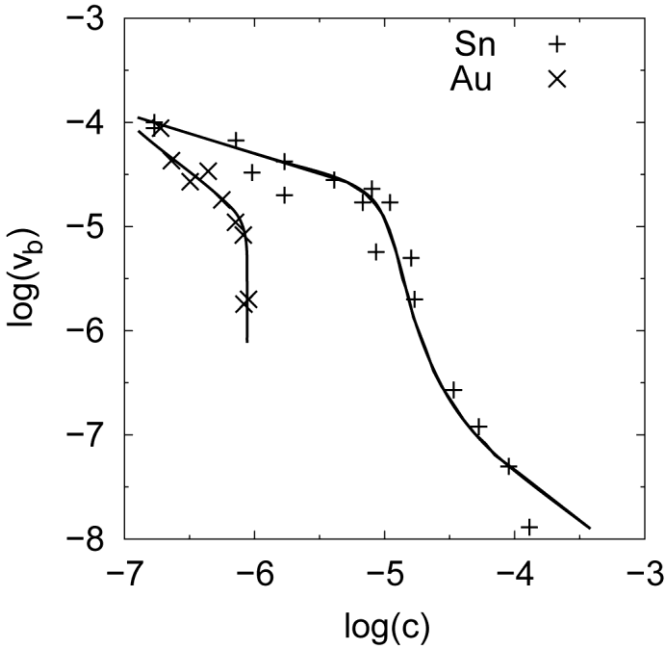

Fig. 2. Comparison of the grain boundary migration rates at 300 °C as a function of solute concentration for tin and gold as solutes in high-purity lead, from Refs. [25] and [26]. The solid lines outline the trend displayed by the experimental points.

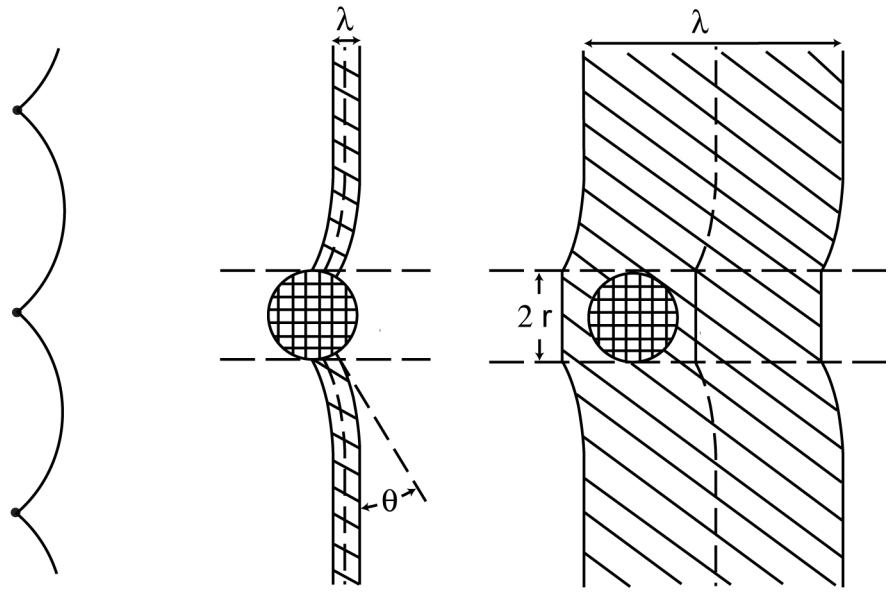

Fig. 3. a) Formation of a cusp on a migrating grain boundary due to interactions with solute atoms (redrawn from Machlin [29]). b) and c) for boundary thickness small and large respectively, compared to the atomic diameter (redrawn from Lücke and Stüwe [10]).

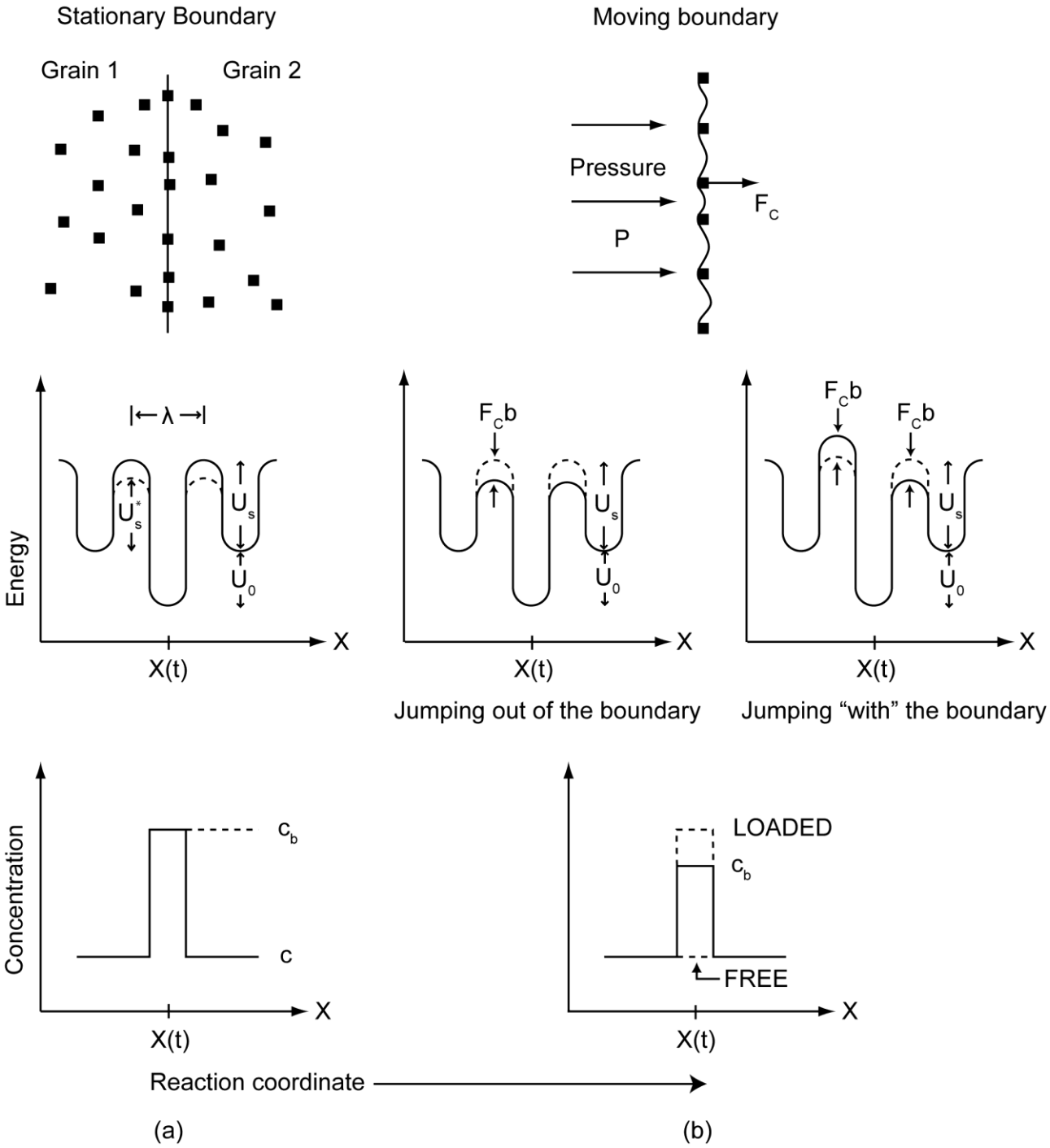

Fig. 4. Schematic representation of the interactions between a) a stationary and b) a migrating grain boundary and solute atoms, for details see the text.

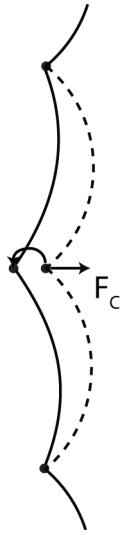

Fig. 5. Schematic representation of an atom jumping against the cusping bias $F_C b$.

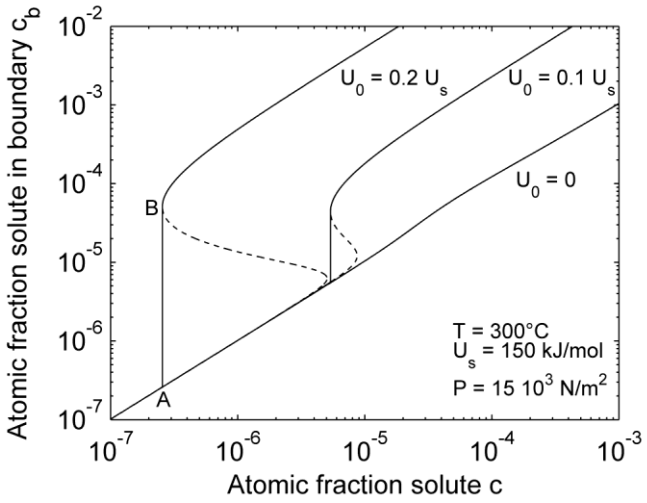

Fig 6a)

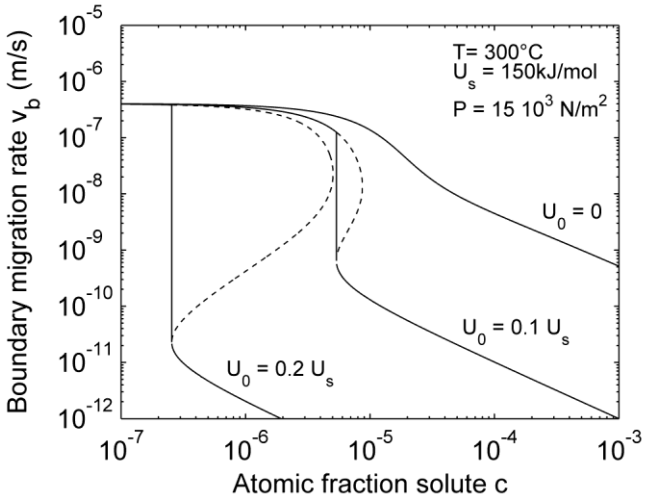

Fig 6b)

Fig. 6. Model predictions for: a) solute atom concentration in the boundary c_b vs. that in the bulk c in a migrating boundary under constant driving pressure, for the U_o-values given b) the corresponding variation in the migration rate v_b.

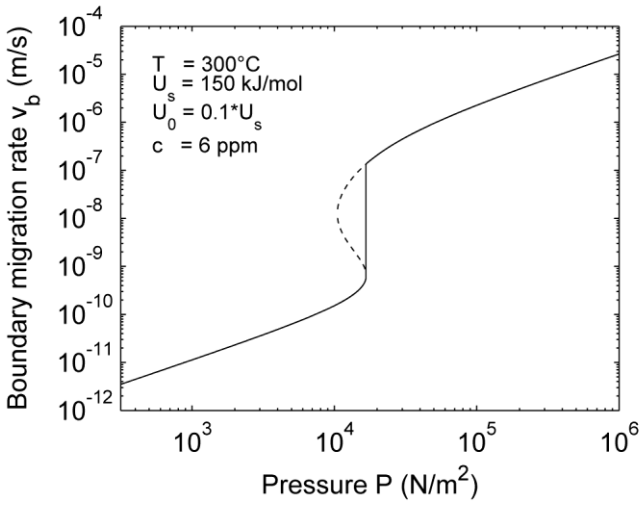

Fig 7a)

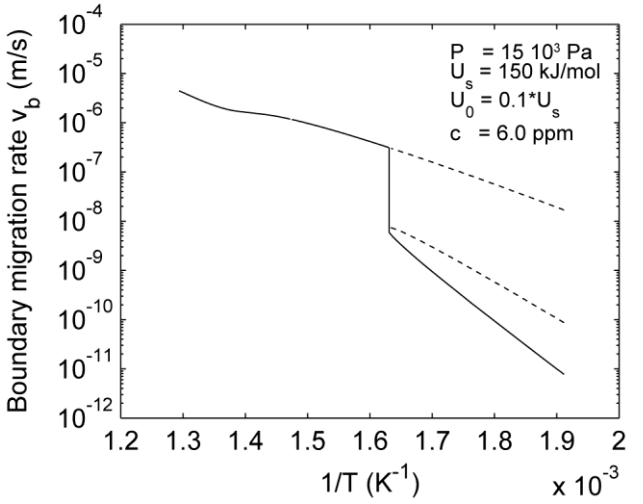

Fig 7b)

Fig. 7. Model predictions for the variations in the boundary migration rate v_b vs. a) the driving pressure *P* and b) the inverse temperature *1/T*.

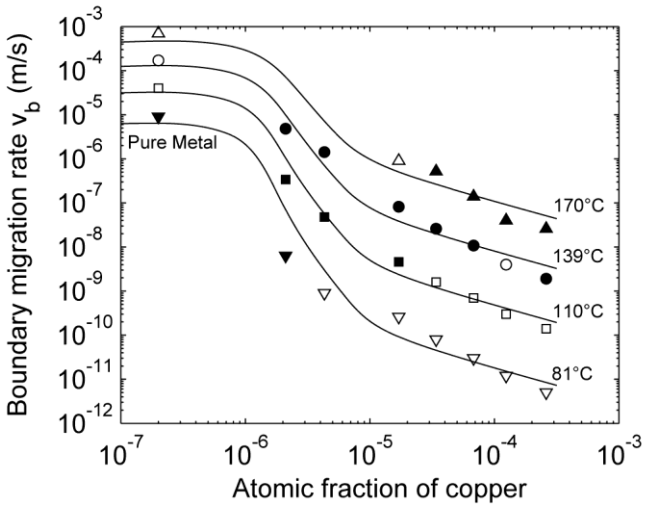

Fig. 8. Experimental [33] and theoretically predicted variation in migration rate vs. composition for the temperatures given (filled symbols, actual data points; open symbols, extrapolated values). As velocities for a pure metal could not be reported in a log-log plot, they have been plotted at an arbitrary abscise of $2\ 10^{-7}$.

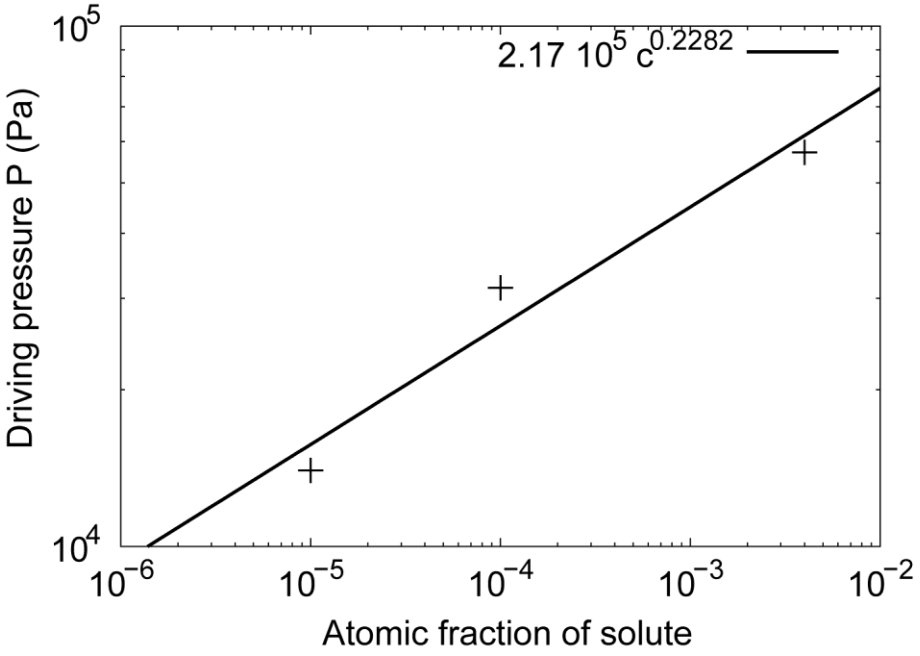

Fig. 9 Variation of the estimated driving force for recrystallisation in function of the purity degree of aluminium.

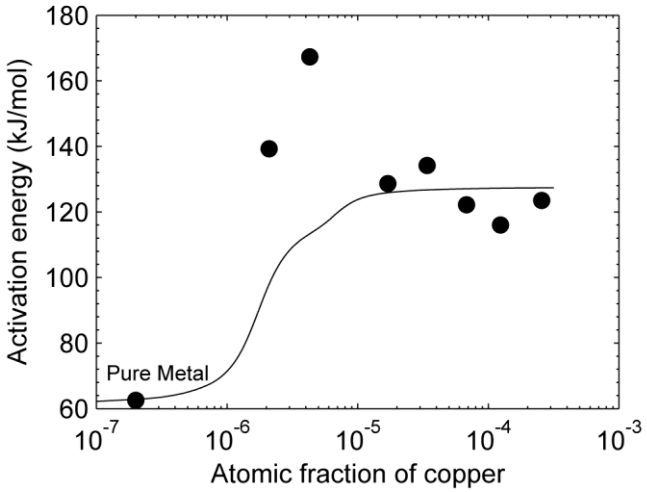

Fig. 10 Activation energy (partially apparent) for boundary migration as a function of atomic fraction of copper, experimental data from Gordon and Vandermeer [33].

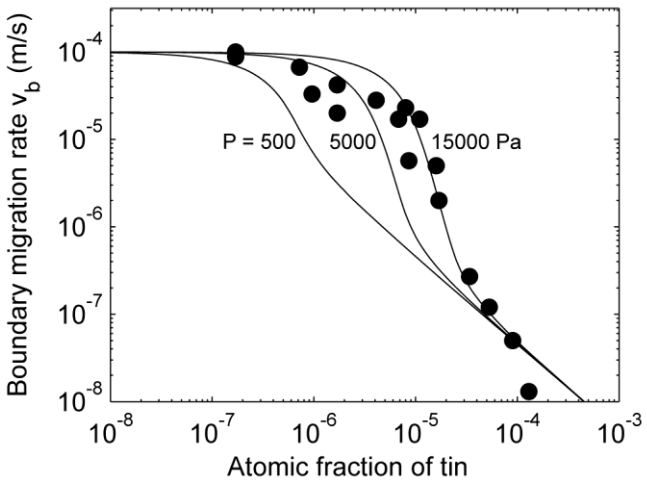

Fig. 11.Model predictions of the boundary migration rate as a function of solute atom concentration for the driving pressures given, as compared to the results on tin in lead by Aust and Rutter [25].

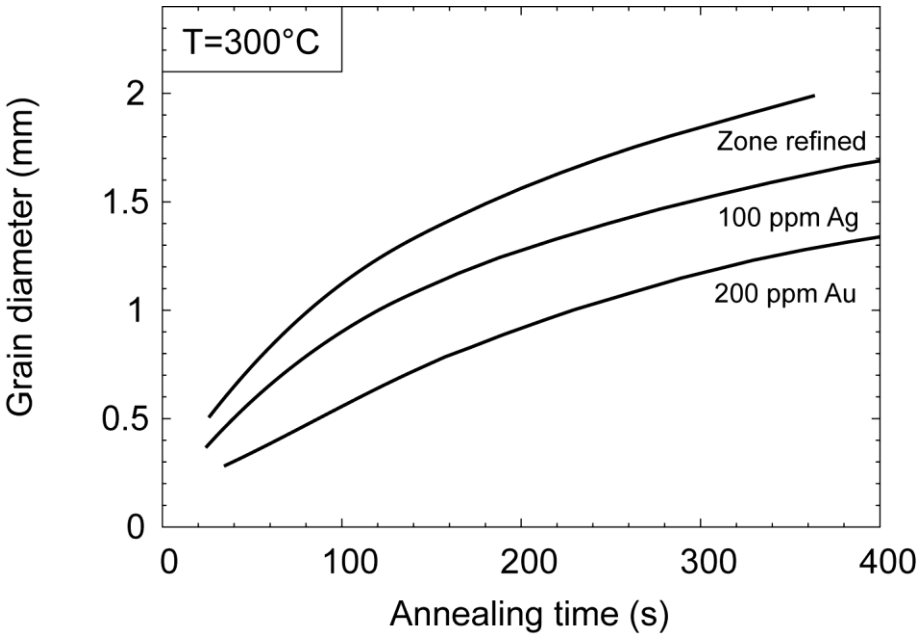

Fig. 12. Grain diameter vs. annealing time at 300 °C for zone-refined lead (top), zone-refined lead with 100 ppm silver added (middle) and zone-refined lead with 200 ppm gold added (bottom), from Bolling and Winegard [39-40].

Tables

Purity of aluminium	$\sigma_{\varepsilon=0.4} - \sigma_0$	$P = \frac{2}{G} \frac{\left(\sigma_{\varepsilon=0.4} - \sigma_0\right)^2}{M^2}$
Commercial purity	85 MPa	$57\,10^3$ Pa
4N	63 MPa	$31\,10^3$ Pa
5N	42 MPa	$14\,10^3$ Pa

Table 1 : Values of the flow stress and the driving pressure for different purity degrees of aluminium at 40% elongation taken from [37]. (G shear modulus in aluminium taken as 26 GPa and M Taylor factor taken as 3).